

ENCIT-2018-0481

THICKNESS INFLUENCE OF THE COPPER POWDER SINTERED CAPILLARY STRUCTURE IN THE THERMAL PERFORMANCE OF HEAT PIPES

Larissa Krambeck¹

Guilherme Antonio Bartmeyer¹

Davi Fusão¹

Paulo Henrique Dias dos Santos²

Thiago Antonini Alves¹

Federal University of Technology – Paraná, ¹Ponta Grossa/PR, ²Curitiba/PR, Brazil

larikrambeck@hotmail.com, gabartmeyer@hotmail.com, davi@utfpr.edu.br, psantos@utfpr.edu.br, thiagoalves@utfpr.edu.br

Abstract. An experimental evaluation of the thermal performance of heat pipes with different thickness of a sintered capillary structure was performed in this research. Due to the geometric characteristics, the manufactured heat pipes can be used in electronics cooling. The heat pipes are used to enhance the heat transfer and are based on phase change. The sintered metal powder structures have a high capillary pumping, low pores, and a good thermal conductivity. The heat pipes were manufactured from a straight copper pipe with the external diameter of 9.45 mm, an inner diameter of 7.75 mm, and a length of 200 mm. The capillary structure was made of sintered copper powder with three different thicknesses (2.125 mm, 1.500 mm, and 0.875 mm). Water was used as the working fluid and the best loading filling ratio of the evaporator volume was developed for each type of capillary structure. The condenser was cooled by air forced convection, the adiabatic section was insulated, and the evaporator was heated by an electrical resistor and was insulated from the environment with aeronautic insulation. The heat pipes were tested at the horizontal under different low heat loads (from 5 up to 45 W). The experimental results showed that all sintered heat pipes worked satisfactorily, however the Type #3 with a filling ratio of 100% showed the best thermal performance when compared with the others.

Keywords: sintered powder, thickness, thermal performance, heat pipe, experimental.

1. INTRODUCTION

The heat pipe is a highly efficient heat transfer passive device that operates on a closed biphasic cycle and uses the latent heat of vaporization of the working fluid to transfer heat from small temperature gradients (Reay *et al.*, 2014). The main advantages of a heat pipe are high thermal conductivity, no need for pumping, no moving parts, and relatively low-pressure drops. The heat pipe consists of an evacuated metal tube, an internal capillary structure, and a working fluid (Krambeck *et al.*, 2017). This device is applied to improve the transfer of heat in many industrial areas, such as electronics, aerospace, telecommunications, food, among others (Faghri, 2014).

The heat pipes operate according to the following principle (Groll and Rösler, 1992): in the evaporator region, heat is transferred to the heat pipe, vaporizing the working fluid contained inside this region. The steam generated is moved, due to the pressure and density differences, to the condenser where heat transported is rejected to the cold source. In the heat rejection process, the steam condenses, and the condensate returns back to the evaporator closing the cycle. The adiabatic region may have variable dimensions or be absent and it is located between the evaporator and the condenser, being insulated from the external environment (Mantelli, 2015). The working fluid returns from the condenser to the evaporator due to capillary pumping effect. A schematic diagram of the operating principle of heat pipes is presented in Fig. 1. More details on the principle of the heat pipes can be found in Chi (1976), Peterson (1994), Faghri (2014), and Reay *et al.* (2014).

The function of the capillary structure is to promote capillary pumping and the way to flow the working fluid. Thus, it directly influences the thermal performance of a heat pipe (Elnaggar, 2014). Capillary structures of sintered metal powders are made from the sintering process, where the powder particles melt resulting in a continuous medium of flow. The sintering is performed by heating the casing tube with the metallic powder particles and the aid of a mandrel. In this way, the metallic powder particles sinter between them and the inner wall of the tube (German, 1994). The mandrel-model is made of a special material so that it is easily removed after the sintering is finished. Sintered capillary structures have a high capillary pumping, low pores, and a good thermal conductivity (Khalili and Shafili, 2016). The main parameters that influence the sintering process are: process time, temperature, particle size, and atmosphere.

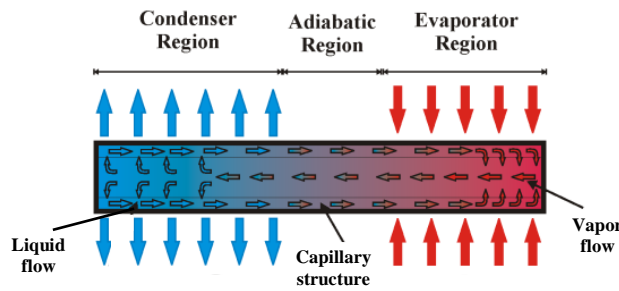


Figure 1. Sketch of the operating principle of a heat pipe

In this research was performed an experimental evaluation of the thermal performance of heat pipes with different thickness of a sintered capillary structure. Due to the geometric characteristics, the manufactured heat pipes can be used in electronics cooling. The heat pipes were produced with spherical copper powder and temporary mandrels, which placed powder in the annulus region. The analyzed operating position was horizontal.

2. METHODOLOGY

The methodology for manufacture (cleaning, assembly, tightness test, evacuation procedure, and filling with the working fluid); tests; and analysis of the heat pipes were developed based on Antonini Alves *et al.* (2018).

2.1 Characteristics of the Heat Pipes

The heat pipes were produced by copper tubes (ASTM B75 Alloy 122) with an outer diameter of 9.45 mm, an inner diameter of 7.75 mm, and a length of 200 mm. The heat pipes have an evaporator region of 80 mm in length, an adiabatic region of 20 mm in length, and a condensation region of 100 mm in length. The capillary structure was made of sintered copper powder with three different thicknesses (2.125 mm, 1.500 mm, and 0.875 mm). Water was used as the working fluid and the best loading filling ratio of the evaporator volume was developed for each thickness. Table 1 presents the main characteristics of heat pipes analyzed in this research.

Table 1. Main characteristics of heat pipes.

Characteristics	Heat Pipe		
	Type #1	Type #2	Type #3
Inner diameter [mm]	7.75	7.75	7.75
Outer diameter [mm]	9.45	9.45	9.45
Thickness of capillary structure [mm]	2.125	1.500	0.875
Evaporator [mm]	80	80	80
Adiabatic section [mm]	20	20	20
Condenser [mm]	100	100	100
Working fluid	Water		
Filling ratio [%]	120	100	100
Volume of working fluid [mL]	3.09	2.83	3.17
Capillary Structure	Sintered Copper Powder		

The sintering process with a copper powder and a temporary mandrel produced the sintered heat pipe. The volume-based average particle diameter of the copper powder is 33 μm (Krambeck *et al.*, 2018). Figure 2 shows a sample of each type of the capillary structures obtained through the sintering process. A micrography of the capillary structure of sintered copper powder is presented in Fig. 3. The image was obtained by Backscattered Electron Detector (BSD) for Scanning Electron Microscope (SEM).

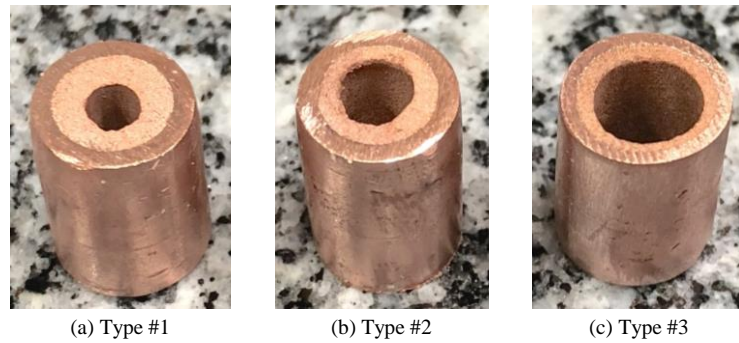


Figure 2. Sample of different configurations of sintered copper powder capillary structures

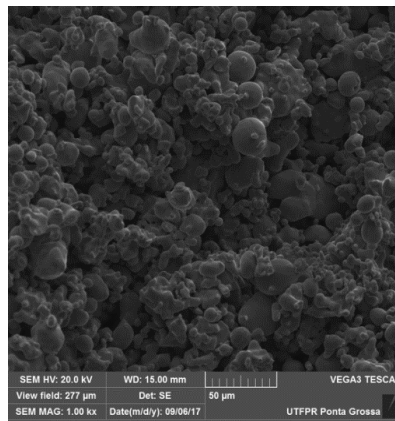


Figure 3. Micrography of the capillary structure.

2.2 Experimental Apparatus

The experimental apparatus used for the experimental tests, shown in Fig. 4, is composed of a power supply unit (Agilent™ U8002A), a data logger (Agilent™ 34970A with 20 channels), a laptop (Dell™), an uninterruptible power supply (NHS™), a universal support, and a fan (Ultrar™).



Figure 4. Experimental apparatus

For the evaluation of the thermal performance of the heat pipes, K-type thermocouples *Omega Engineering*™ were used. They were fixed on the outer surface of the heat pipe by a thermosensitive adhesive strip *Kapton*™. As shown in Fig. 5, there were three thermocouples in the evaporator ($T_{evap,1}$, $T_{evap,2}$, and $T_{evap,3}$), one thermocouple in the adiabatic section (T_{adiab}) e four thermocouples in the condenser ($T_{cond,1}$, $T_{cond,2}$, $T_{cond,3}$, and $T_{cond,4}$) in heat pipes.

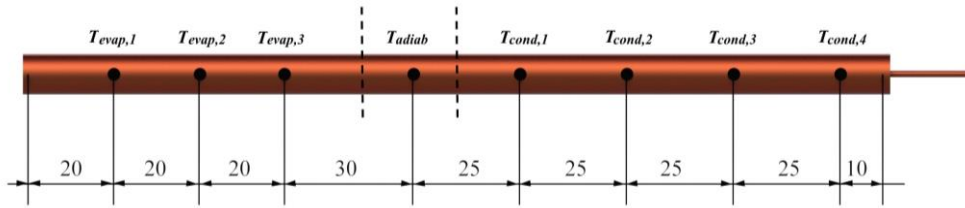


Figure 5. Thermocouple positions [mm]

The heating system of the evaporator is conducted by power dissipation from the passage of an electric current in a nickel-chromium alloy power strip resistor *Omega Engineering*TM with 0.1 mm of thickness and 3.5 mm of width. To ensure that the generated heat by Joule effect is transmitted to the evaporator, an aeronautic thermal insulation and a layer of polyethylene are installed in this region. A fiberglass tape is used in adiabatic section as heat insulation between the support and the heat pipe. The cooling system using air forced convection consisted of a fan in the condenser region.

2.3 Experimental Procedure

To ensure the best results and the repeatability of experimental tests, the ambient temperature was maintained at $20^{\circ}\text{C} \pm 1^{\circ}\text{C}$. A thermal conditioning system *Carrier*TM was used for this purpose. A detailed check of the equipment and the heat pipe (fixing thermocouples, thermal insulation, resistor connection, among others) must be made before each experimental test. The heat pipe was carefully fixed to the universal support bracket in the adiabatic region in the desired position. The cooling system was turned on in the condenser region and set at a speed of 5m/s controlled by a potentiometer with a combined error of $\pm 0.2\text{m/s}$. The data acquisition system was turned on, collecting the temperatures measured by the K-type thermocouples. The temperatures should be verified according to the ambient temperature, and if these were stable and approximately 20°C , finally, the heating system can be turned on and adjusted to the dissipation power desired. The initial load was 5W and, after approximately 15 minutes, the thermocouples showed stationary values. If it happened, the thermal load has been increased by 5W. The load increment was made until the maximum temperature of the device reached the critical temperature (160°C), where the melting of the materials could happen. Data were acquired every 5 (five) seconds, recorded in the desktop by the software *Agilent*TM *Benchlink Data Logger 3*.

2.4 Data Reduction

The thermal performance of the heat pipes was analyzed and compared by the operating temperature (T_{op}) and the global thermal resistance (R_{th}). The analyzed operating temperature is the temperature of the adiabatic region. The global thermal resistance, R_{th} , of a heat pipe can be defined as the difficulty of the passive device to transport the heat power and can be calculated by:

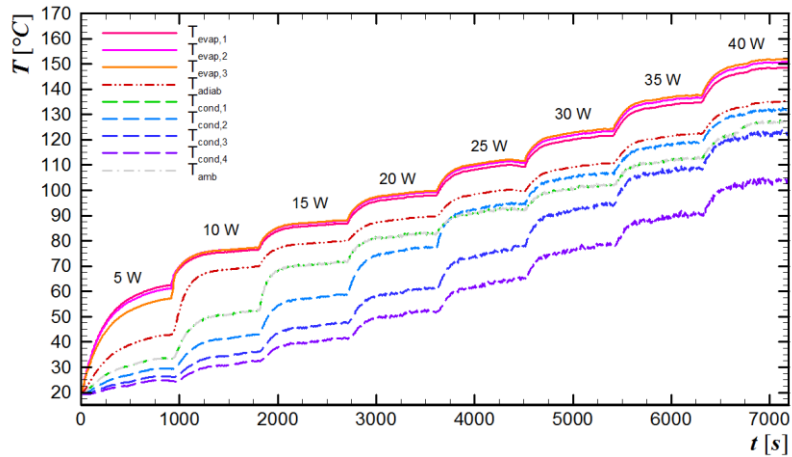
$$R_{th} = \frac{\Delta T}{q} = \frac{(T_{evap} - T_{cond})}{q} \quad (1)$$

where, q is the heat transfer capability of the device, T_{evap} and T_{cond} are the mean temperature of the evaporator and the condenser, respectively.

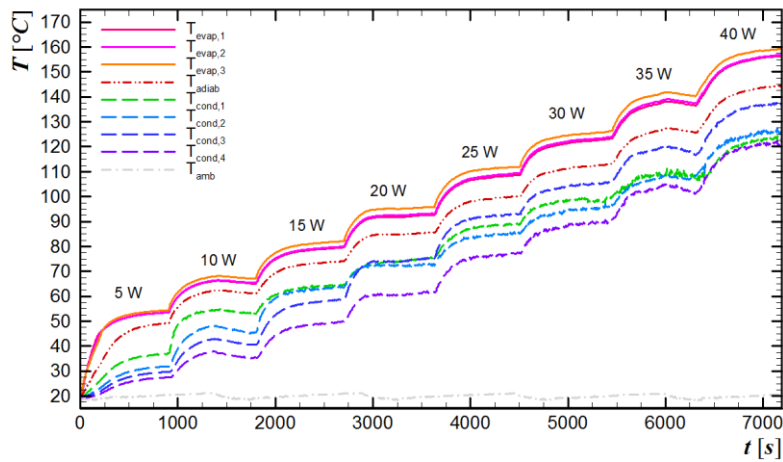
The uncertainties of the measurements were estimated for the temperature and heat load. Taking into account the accuracy of the temperature sensors (K-type thermocouples) and the uncertainties of the data logger, the uncertainty of the measured temperatures were estimated at $\pm 1.27^{\circ}\text{C}$. The uncertainty of the electrical power input was estimated at $\pm 1\%$ including the uncertainty of the power supply unit and the uncertainty of the data logger. The uncertainties are shown in the obtained results. For the correlated uncertainties determination, the error propagation method described by Holman (2011) was used.

3. RESULTS AND DISCUSSION

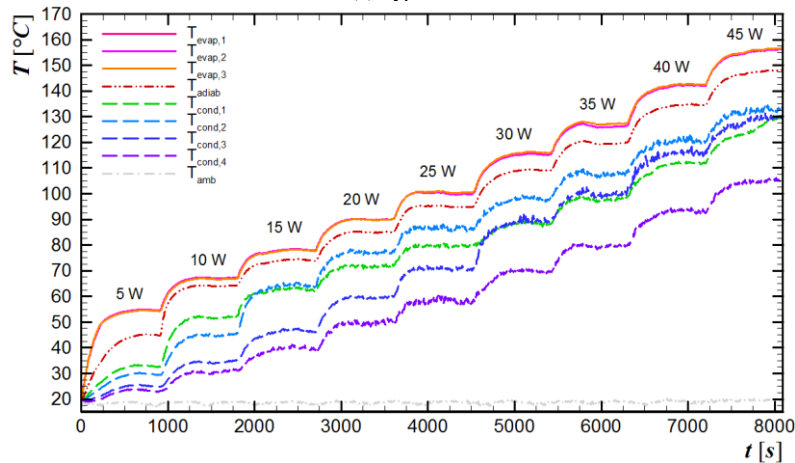
The experimental results regarding the thermal behavior of the heat pipes with different thickness of the capillary structure are presented. The experimental tests were repeated three times and the errors were compared considering the difference between the mean values less than 0.5°C . The tests were performed at increasing heat loads of 5W, ranging from 5 to 45W for the horizontal position. Figure 6 shows the temperature distributions as a function of time for the three types of the heat pipe in the horizontal position.



(a) Type #1



(b) Type #2



(c) Type #3

Figure 6. Temperature distribution *versus* time of the heat pipes

The behavior of the operating temperature as a function of the dissipated power for different heat pipes is shown in Figure 7. It may be noted that as the dissipated power increases, the operating temperature also increases for all the types of sintered heat pipes. By comparing the best filling ratios of each type, it is possible to verify that the behaviors of the heat pipes are very similar. In general, the operating temperatures ranged from 40°C to 145°C. In addition, all types supported a power of at least 40W. Thus, according to the operating temperature, for thermal loads of up to 40W we could use any pipe configuration. However, if the application requires a power dissipation of 45W, Type #3 would be the most appropriate.

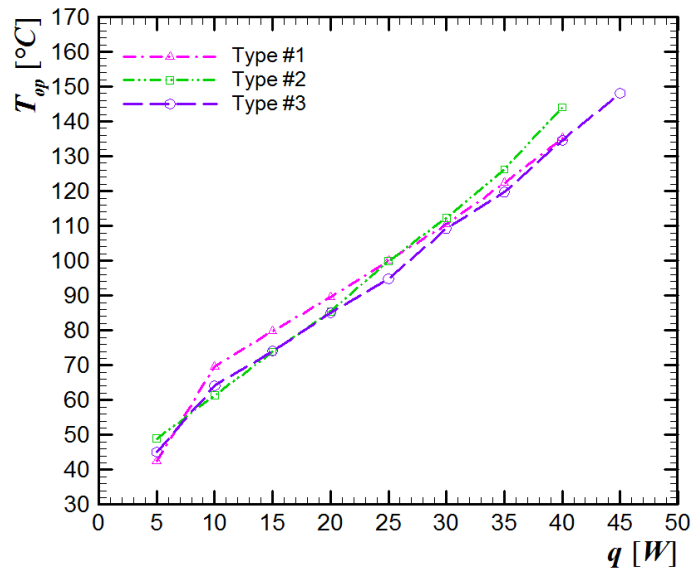


Figure 7. Operating Temperature *versus* power dissipation

Figure 8 presents the global thermal resistance as a function of the power dissipation considering the three thickness of the sintered capillary structure. As the heat dissipation is increased, the thermal resistance decreases for the heat pipes in the horizontal position. The thermal resistances are very similar and present satisfactory performances. Thermal resistances range from 6.5°C/W to 0.5°C/W.

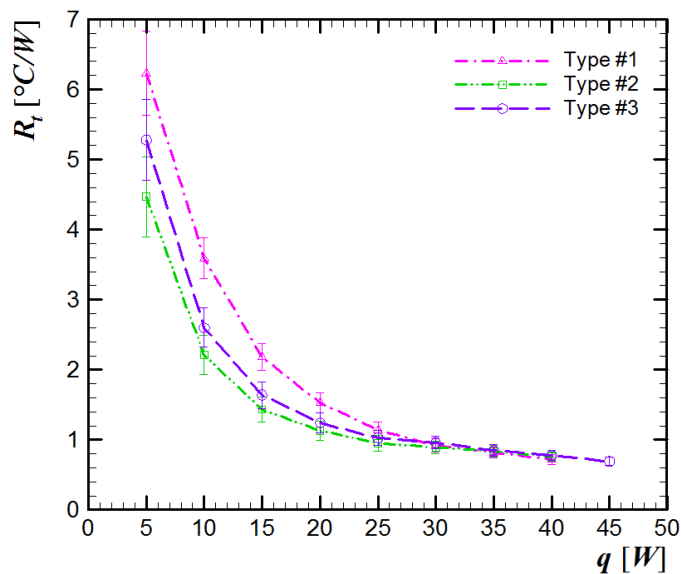


Figure 8. Thermal resistance *versus* power dissipation

The experimental results showed that all sintered heat pipes worked satisfactorily, however the Type #3 with a filling ratio of 100% showed the best thermal performance when compared with the others because can support a higher power dissipation.

4. CONCLUSIONS

In this research was performed an experimental evaluation of the thermal performance of heat pipes with different thickness of a sintered capillary structure. Due to the geometric characteristics, the manufactured heat pipes can be used in electronics cooling. The heat pipes were tested horizontally under different low heat loads (from 5 up to 45W). Water was used as the working fluid and the best loading filling ratio of the evaporator volume was developed for each type of capillary structure. As a result of the study, all the sintered heat pipes worked successfully, however the Type #3 with a filling ratio of 100% showed the best thermal performance when compared with the others.

5. ACKNOWLEDGEMENTS

Acknowledgments are provided to the Capes, the CNPq, the PROPPG/UTFPR, the DIRPPG/UTFPR, the PPGEM/UTFPR/Ponta Grossa, and the DAMEC/UTFPR/Ponta Grossa.

6. REFERENCES

- Antonini Alves, T., Krambeck, L. and Santos, P.H.D., 2018. "Heat Pipe and Thermosyphon for Thermal Management of Thermoelectric Cooling". In: ARANGUREN, Patricia. *Bringing Thermoelectricity into Reality*. 1st Ed. London: InTech, Cap. 17. p. 353-374.
- Chi, S.W., 1976. *Heat Pipe Theory and Practice: A Sourcebook*. Hemisphere Publishing Corporation, Washington, USA.
- Elnaggar, M.H.A., 2014 "The Optimization of Thickness and Permeability of Wick Structure with Different Working Fluids of L-Shape Heat Pipe for Electronic Cooling". *Jordan Journal of Mechanical and Industrial Engineering*, Vol. 8, no. 3, pp. 119-125.
- German, R.M., 1994. "Powder Metallurgy Science". *Metal Powder Industry Federation*, New Jersey, USA, 472p.
- Groll, M. and Rösler, S., 1992. "Operation Principles and Performance of Heat Pipes and Closed Two-Phase Thermosyphons". *Journal of Non-Equilibrium Thermodynamics*, Vol. 17, pp. 091-151.
- Holman, J.P., 2011. *Experimental Methods for Engineers*. Mcgrall-Hill, Singapore.
- Faghri, A., 2014. "Heat Pipes: Review, Opportunities and Challenges". *Frontiers in Heat Pipes*, Vol. 5, pp 01-48.
- Khalili, M. and Shafili, M.B., 2016. "Experimental and Numerical Investigation of the Thermal Performance of a Novel Sintered-Wick Heat Pipe". *Applied Thermal Engineering*, Vol. 94, pp. 59-75.
- Krambeck, L., Bartmeyer, G.A., Fusão, D., Santos, P.H.D. and Antonini Alves, T., 2018. "Desempenho térmico de um tubo de calor utilizando pó de cobre sinterizado como estrutura capilar". In *Anais do X Congresso Nacional de Engenharia Mecânica – CONEM 2018*. Salvador, Brazil.
- Krambeck, L., Nishida, F.B., Santos, P.H.D. and Antonini Alves, T., 2017. "Heat pipe with axial microgrooves fabricated by wire electrical discharge machining (wire-EDM)". In *Proceedings of the 9th World Conference on Experimental Heat Transfer, Fluid Mechanics and Thermodynamics – ExHFT 2018*. Foz do Iguaçu, Brazil.
- Mantelli, M.B.H., *Tubos de Calor e Termossifões*, Notas de Aula, Departamento de Engenharia Mecânica, Universidade Federal de Santa Catarina, Florianópolis, SC, Brasil, 2015.
- Peterson, G.P., 1994. *An Introduction to Heat Pipes: Modeling, Testing and Applications, (Thermal Management of Microelectronic and Electronic System Series)*. Wiley-Interscience, New York, USA.
- Reay, D.A., Kew, P.A. and McGlen, R.J., 2014. *Heat Pipe: Theory, Design and Applications*. Butterworth-Heinemann, Amsterdam, NED.

7. RESPONSIBILITY NOTICE

The authors are the only responsible for the printed material included in this paper.